

NASA Technical Memorandum 102362  
ICOMP-89-26

# Wall-Layer Eruptions in Turbulent Flows

J.D.A. Walker  
*Lehigh University*  
*Bethlehem, Pennsylvania*

*and Institute for Computational Mechanics in Propulsion*  
*Lewis Research Center*  
*Cleveland, Ohio*

September 1989



(NASA-TM-102362) WALL-LAYER ERUPTIONS IN  
TURBULENT FLOWS (NASA) 13 p CSCL 200



N90-11250

Unclass  
G3/34 0234683



## WALL-LAYER ERUPTIONS IN TURBULENT FLOWS

J.D.A. Walker

Department of Mechanical Engineering and Mechanics  
Lehigh University, Bethlehem, PA 18015

and Institute for Computational Mechanics in Propulsion\*  
Lewis Research Center, Cleveland, Ohio 44135

### ABSTRACT

The near-wall region of a turbulent flow is investigated in the limit of large Reynolds numbers. When low-speed streaks are present, the governing equations are shown to be of the boundary-layer type. Physical processes leading to local breakdown and a strong interaction with the outer region are considered. It is argued that convected vortices, predominantly of the hairpin type, will provoke eruptions and regenerative interactions with the outer region.

### 1. Introduction

Most flows occurring in engineering practice are turbulent and at high Reynolds number. The study of the dynamics of turbulent boundary layers is therefore an important area of basic research. However, analysis is extremely difficult due to the complex unsteady environment which contains a rich mixture of scales and three-dimensional vortex structures; the vortices interact with one another and with the viscous flow near solid walls. The interaction with the near-wall flow is the fundamental process of turbulence production whereby the turbulence is sustained. The wall layer is observed to erupt intermittently, at isolated streamwise and spanwise locations, in an event usually referred to as bursting. In this process new vorticity from the wall is abruptly introduced into the outer region of the boundary layer. In a turbulent boundary layer, the only source of new vorticity is the wall and thus the important issues of regeneration are necessarily related to the surface interaction. The nature of this interaction and the physical processes involved are the subject of this paper.

The mean turbulent boundary layer is double-structured consisting of: (1) an outer layer where the balance in the mean equations is between convection and Reynolds stress, and (2) an inner wall layer having constant total stress, where viscous and Reynolds stress terms balance and the convective terms are not important to leading order. A significant consequence of the observed<sup>1</sup> coherent structure of the near-wall region (see Walker et al<sup>2</sup> and the references therein) is that the mean normal length scale is also appropriate for the time-dependent flow over relatively long periods of time. For a given area of the surface, the wall layer will be observed to be in a relatively quiescent state for a large majority of the total observation time<sup>1,2</sup>. During this quiescent period, the low-speed streaks can be observed, the flow is relatively well-ordered and strong interactions with the outer region do not occur. In this state, the wall layer is a relatively thin viscous region and may be regarded as a developing unsteady flow, driven by the pressure field at the base of the outer region. Indeed, a plausible cause of the wall-layer streaks is that they are the signature of convected hairpin vortices<sup>2,3,4</sup>.

The relatively long periods of ordered flow are interrupted on a highly intermittent basis at isolated locations by the bursting phenomenon. The

---

\*Work funded under Space Act Agreement C99066G.

event invariably initiates near a wall-layer streak<sup>2</sup> and is characterized by an abrupt and highly localized eruption of wall-layer fluid. The process may be classified as a strong unsteady viscous-inviscid interaction or equivalently, as a local breakdown of the wall-layer flow. During the relatively short period of breakdown, the two regions of the boundary layer interact strongly and the double structure of the layer is briefly obliterated. In the process, new vorticity from the wall is abruptly introduced into the outer region. A double structure is quickly restored locally with the sweep event, in which high speed outer-region fluid penetrates close to the wall following the burst; the low-speed streaks appear again and locally a new quiescent state begins.

A central question relates to what dynamical features cause the local breakdown of the wall-layer flow. The most productive theoretical approach is to identify cause and effect relationships in the limit of large Reynolds numbers, for several reasons. First, most practical flows occur at high Reynolds numbers and it is desirable to construct an asymptotic description which represents the phenomena over a range of Reynolds numbers. Secondly, the structure of high speed compressible turbulent flows is expected to be similar to the well-studied incompressible case; detailed experimental studies become progressively more difficult with increasing flow speed and a knowledge of the dominant dynamical mechanisms at high Reynolds number provides the basis of an extension to high Mach number flows. The theoretical task is difficult since most of the experimental work is in a limited Reynolds number range; in addition, the complexity of the unsteady environment suggests a multitude of different physical cause and effect relationships. The task in constructing an asymptotic description is to isolate the scales and dominant processes at high Reynolds numbers. Direct simulations of turbulent flows are less helpful in this objective than detailed experimental studies; simulations are currently restricted to relatively low Reynolds numbers and seem to lack the numerical resolution and methodology to adequately describe the eruptive phenomena of interest here. In the next section, the scaled variables describing an evolving quiescent wall-layer flow are developed.

## 2. The Wall Layer Problem

Consider a nominally steady two-dimensional boundary layer and let  $u_\tau(x)$  be the local mean friction velocity. During a typical quiescent period, the wall layer is well-defined and the low-speed streaks are present; all three velocity components are  $O(u_\tau)$  and the characteristic length in the spanwise direction is  $\lambda$ , the mean streak spacing. First define a scaled coordinate and velocity in the spanwise direction by

$$Z = u_\tau z / (\lambda^+ \nu) = z / \lambda, \quad W = w / (u_\tau W_1), \quad (1)$$

where  $\lambda^+$  is observed<sup>5</sup> to have a value of about 100; here  $\nu$  is the kinematic viscosity and  $W_1$  is a constant, such that  $W_1 u_\tau$  is equal to the average magnitude of the spanwise velocity near the outer edge of the wall layer during a typical quiescent state. Measurements of the intensity  $\overline{w'^2}$  for large  $y^+$  ( $y^+ \approx 40-100$ ) indicate an average value of  $W_1$  of about 2. The scaled normal velocity and distance from the wall are defined by

$$Y = u_\tau y (W_1 / \lambda^+)^{1/2} / \nu = y^+ (W_1 / \lambda^+)^{1/2}, \quad V = v (\lambda^+ / W_1)^{1/2} / u_\tau, \quad (2)$$

which follow from balancing: (1)  $\partial v / \partial y$  and  $\partial w / \partial z$  in the continuity equation and (2) the convective operator  $v \partial / \partial y$  with the viscous operator  $\nu \partial^2 / \partial y^2$  in the momentum equations. A scaled streamwise coordinate and velocity are

defined by

$$x = x/L_x, \quad U = u/(U_1 u_\tau) \quad (3)$$

Here  $L_x$  is the characteristic length in the streamwise direction, whose value will be discussed subsequently;  $U_1$  is a constant such that  $U_1 u_\tau$  is a typical average flow speed in the streamwise direction near the outer edge of the wall layer during the quiescent period. Typical  $U_1$  values of 13-16 can be estimated from the law of the wall for  $y^+ = 30-100$  and consequently  $U_1$  is generally considerably larger than  $W_1$ . The time scale follows from a balance between the time derivative and normal viscous diffusion terms and let

$$T = u_\tau^2 t W_1 / (\nu \lambda^+) = t^+ W_1 / \lambda^+ \quad (4)$$

Finally the pressure may be written as

$$p = p_\infty(x) + \rho u_\tau^2 U_1^2 p_1 + \rho u_\tau^2 U_1 W_1 p_2 / \lambda^+ + \dots \quad (5)$$

where  $p_\infty(x)$  is the mainstream pressure and  $\rho$  is the density. Upon substitution in the continuity equation, it is easily shown that

$$\frac{\gamma}{Re_x} \frac{\partial U}{\partial X} + \frac{\partial V}{\partial Y} + \frac{\partial W}{\partial Z} = 0 \quad (6)$$

Here  $Re_x$ , a streamwise Reynolds number, and the parameter  $\gamma$  are defined by

$$Re_x = u_\tau L_x / \nu, \quad \gamma = \lambda^+ U_1 / W_1 \quad (7)$$

Substitution in the Navier-Stokes equations yields

$$\begin{aligned} \frac{\partial U}{\partial T} + \frac{\gamma}{Re_x} U \frac{\partial U}{\partial X} + V \frac{\partial U}{\partial Y} + W \frac{\partial U}{\partial Z} &= \frac{\lambda^+}{U_1 W_1} p^+ - \frac{\gamma}{Re_x} \frac{\partial p_1}{\partial X} - \frac{1}{Re_x} \frac{\partial p_2}{\partial X} \\ &+ \frac{\gamma}{U_1 Re_x^2} \frac{\partial^2 U}{\partial X^2} + \frac{\partial^2 U}{\partial Y^2} + \frac{1}{Re_\lambda} \frac{\partial^2 U}{\partial Z^2}, \end{aligned} \quad (8)$$

$$\begin{aligned} \frac{\partial V}{\partial T} + \frac{\gamma}{Re_x} U \frac{\partial V}{\partial X} + V \frac{\partial V}{\partial Y} + W \frac{\partial V}{\partial Z} &= -\gamma U_1 \frac{\partial p_1}{\partial Y} - U_1 \frac{\partial p_2}{\partial Y} \\ &+ \frac{\gamma}{U_1 Re_x^2} \frac{\partial^2 V}{\partial X^2} + \frac{\partial^2 V}{\partial Y^2} + \frac{1}{Re_\lambda} \frac{\partial^2 V}{\partial Z^2}, \end{aligned} \quad (9)$$

$$\begin{aligned} \frac{\partial W}{\partial T} + \frac{\gamma}{Re_x} U \frac{\partial W}{\partial X} + V \frac{\partial W}{\partial Y} + W \frac{\partial W}{\partial Z} &= -\frac{U_1^2}{W_1} \frac{\partial p_1}{\partial Z} - \frac{U_1}{Re_\lambda} \frac{\partial p_2}{\partial Z} \\ &+ \frac{\gamma}{U_1 Re_x^2} \frac{\partial^2 W}{\partial X^2} + \frac{\partial^2 W}{\partial Y^2} + \frac{1}{Re_\lambda} \frac{\partial^2 W}{\partial Z^2}. \end{aligned} \quad (10)$$

Here  $p^+$  is the scaled mainstream pressure gradient defined by

$$p^+ = -v(dp_\infty/dx)/(\rho u_\tau^3), \quad (11)$$

and  $Re_\lambda$  is a spanwise Reynolds number defined by

$$Re_\lambda = W_1 \lambda^+ = W_1 u_\tau \lambda / \nu. \quad (12)$$

This completes the formulation with a minimum number of assumptions. Length and velocity scales consistent with experiment have been introduced to describe a developing wall-layer flow containing low-speed streaks. The objective now is to isolate the type of disturbance which can induce a local wall-layer breakdown and interaction with the outer flow. In the next two sections, several limit problems are considered, all for large streamwise Reynolds number  $Re_x$ .

### 3. The Long Wave Limit

Consider first the limit

$$Re_x \rightarrow \infty, \quad (\gamma/Re_x) \rightarrow 0, \quad (13)$$

which implies from equation (7) that  $(U_1 \lambda)/(W_1 L_x) \ll 1$ . Thus motion of relatively long streamwise extent with respect to the streak spacing is of interest. It is easily verified that in this limit, equations (6), (9) and (10) involve only the flow components  $(V, W)$  in the cross-flow plane. The streamwise vorticity develops independently in the  $YZ$  plane and the solution for  $V$  and  $W$  then feeds into equation (8), thereby influencing the evolution of  $U$ . Solutions of the long wave equations have been considered by Walker and Herzog<sup>6</sup> subject to the boundary conditions

$$W = V = 0 \quad \text{at} \quad Y = 0, \quad W \rightarrow -\sin(2\pi Z) \quad \text{as} \quad Y \rightarrow \infty. \quad (14)$$

This is the simplest external condition which leads to the representative flow structure depicted in figure 1. A similar set of equations have been studied by other authors<sup>7,8</sup>, with the exception that a periodic time-dependence was assumed in  $W$  at large  $Y$ ; in these studies, the spanwise velocity for large  $Y$  reverses direction during the interval under consideration. The outer condition (14) is similar to that imposed by a moving hairpin vortex on the flow near the wall<sup>9</sup>; it represents a persistent pumping action at the outer edge of the wall layer and is therefore believed to be a more realistic external condition.

In the limit (13) equations (8), (9), (10) contain the Reynolds number  $Re_\lambda$ ; with average values of  $\lambda^+ \approx 100$ ,  $W_1 = 2$ , a typical value of  $Re_\lambda$  is 200. Walker and Herzog<sup>6</sup> have obtained numerical solutions over a range of  $Re_\lambda$ , using an abrupt imposition of (14) at the start of a typical quiescent state; two routes to breakdown of the flow structure depicted in figure 1 were identified. The first occurs in situations where the spanwise velocity at the wall-layer edge produces a relatively strong pumping action, so that  $W_1$ , and hence  $Re_\lambda$ , is large. In such cases, the adverse pressure gradient due to (14) causes the development of recirculating flow near  $Z=0$ ; the evolution in the cross-flow plane is then similar to known examples of vortex-induced separation<sup>10</sup>. Violent updrafts begin to evolve near the recirculating flow, in a region which becomes progressively narrower as the wall layer focuses toward an eruption. This unsteady separation effect will occur whenever a hairpin vortex is close to the wall and/or has a relatively large strength, thus giving rise to elevated levels of  $W_1$ . As the strength of the pumping action is decreased (and with it  $Re_\lambda$ ),

recirculations do appear in the cross-flow plane but the tendency toward a focussed eruption gradually diminishes; at low enough  $Re_\lambda$ , the  $(V, W)$  motion evolves toward an apparently steady state. However, the streamwise velocity profiles were observed<sup>6</sup> to develop a strong inflectional character near the center of the recirculation in the cross-flow plane; the configuration is expected to be highly unstable and to breakdown. This is the second physical process which can lead to the destruction of the assumed flow structure depicted in figure 1. Finally at sufficiently low values of  $Re_\lambda$ , cross-flow separation or inflectional streamwise profiles do not develop. The overall implication of these results<sup>6</sup> is that a sufficiently large level of imposed spanwise velocity at the wall-layer edge is required to produce a breakdown of the structure shown in figure 1.

#### 4. The Full Three-Dimensional Problem

Now consider the limits

$$Re_x \rightarrow \infty, \quad (\gamma/Re_x) = O(1), \quad (15)$$

and without loss of generality take  $\gamma = Re_x$ ; this is equivalent to selecting the characteristic streamwise length according to

$$L_x = U_1 \lambda / W_1. \quad (16)$$

Using the typical values of  $U_1$  and  $W_1$ , equation (16) suggests a characteristic streamwise dimension of 6 to 8 times the spanwise streak spacing, which is consistent with observation<sup>1,2</sup>. It now follows from equation (8) that  $\partial P_1 / \partial Y = O(Re_x^{-1})$  and therefore  $P_1 = P_1(X, Z, T)$ . Equations (8), (10) and (6) become, respectively

$$\frac{\partial U}{\partial T} + U \frac{\partial U}{\partial X} + V \frac{\partial U}{\partial Y} + W \frac{\partial U}{\partial Z} = \frac{\lambda^+ P_1^+}{U_1 W_1} - \frac{\partial P_1}{\partial X} + \frac{\partial^2 U}{\partial Y^2} + \frac{1}{Re_\lambda} \frac{\partial^2 U}{\partial Z^2}, \quad (17)$$

$$\frac{\partial W}{\partial T} + U \frac{\partial W}{\partial X} + V \frac{\partial W}{\partial Y} + W \frac{\partial W}{\partial Z} = - \frac{U_1^2}{W_1^2} \frac{\partial P_1}{\partial Z} + \frac{\partial^2 W}{\partial Y^2} + \frac{1}{Re_\lambda} \frac{\partial^2 W}{\partial Z^2}, \quad (18)$$

$$\frac{\partial U}{\partial X} + \frac{\partial V}{\partial Y} + \frac{\partial W}{\partial Z} = 0. \quad (19)$$

With  $P_1$  assumed known from a specified disturbance flow in the outer region (as well as  $U$  and  $W$  for large  $Y$ ), it is evident that equations (17)-(19) are of the boundary-layer type. Once again  $Re_\lambda$  appears as a parameter and solutions can be considered over a range of  $Re_\lambda$ . Note that in the limit  $Re_\lambda \rightarrow \infty$ , equations (17)-(19) give the three-dimensional "laminar boundary-layer equations". An important consequence of this section is that disturbances which induce eruptions in laminar flows will also (when properly scaled) have the same effect on the turbulent wall layer. Recent computational and experimental studies<sup>3,4,11</sup> strongly suggest that the dominant disturbance near the wall in a turbulent boundary layer is the convected hairpin vortex. In the next section the general effects of convected vortex motion are discussed.

#### 5. The Effects of Moving Vortices

In §3 and §4, it has been demonstrated that during the quiescent period the leading-order wall-layer equations are of the boundary-layer type; the

pressure, as well as the external spanwise and streamwise velocity distributions drive the motion therein, until ultimately an interaction is induced with the outer flow. The question now is what type of convected disturbance can induce an eruption of the wall layer and what are the relevant dynamics? It is argued elsewhere<sup>9,11</sup> that the principal dynamical feature is the hairpin vortex. To understand the effects of such a vortex, it is worthwhile to review some aspects of vortex motion.

As a consequence of a number of fundamental studies, it has been possible to identify the general effect of a moving vortex on a viscous flow near a wall. These studies include two-dimensional vortices in an otherwise stagnant flow above a wall<sup>10</sup>, vortices convected in a uniform flow<sup>12</sup>, counter-rotating vortex pairs<sup>13,14</sup>, vortex rings and loops near a surface<sup>15,16</sup> and moving hairpin vortices<sup>3,4,11</sup>. As each vortex convects near a solid surface, a variety of complex unsteady flow patterns is induced in the viscous flow near the wall. However, a common feature is that a vortex always impresses a region of adverse pressure gradient on the near-wall flow, which ultimately provokes an eruption. Consider the configuration shown in figure 2(a) where a portion of a three-dimensional vortex is in motion above a wall. In figure 2(b) the local detail in a plane normal to the vortex core is depicted. For the indicated sense of rotation, a region of deceleration occurs upstream; this is followed by a zone of acceleration and adverse pressure gradient behind the vortex. In a frame of reference moving with the vortex (at  $x=0$ ), a sketch of the pressure gradient induced near the wall is shown in figure 3. The critical aspects are: (1) the distance of the vortex center  $a$  from the wall; (2) the vortex strength  $\kappa$  and (3) the vortex Reynolds number  $R_v = 2\pi\kappa/\nu$ . The size of the vortex core plays no significant role in the nature of the induced flow near the wall. For large vortex Reynolds numbers, the viscous flow near the wall is only able to withstand the action of the adverse pressure gradient for a finite period of time. In most situations<sup>10,15</sup> a secondary recirculating eddy evolves in the near-wall flow with the opposite sense of circulation to the parent vortex. The important consequence is a blocking effect which develops as the near-wall flow is forced to flow up and over the secondary eddy, under the continued action of the external pressure gradient. Strong updrafts then develop on the upstream side of the secondary eddy causing a violent outflow from a zone that is narrow in the streamwise direction. In the latter stages of the process, the near-wall focuses into an explosively growing needle-like region<sup>10</sup> containing relatively high levels of vorticity. At this point, the near-wall flow erupts and a strong unsteady viscous-inviscid interaction ensues, culminating in the ejection of fluid from the wall region. The pressure response near the wall becomes quite complex as the interaction develops and a typical behavior in the pressure gradient is sketched as a broken line in figure 3, near the point of eruption<sup>17,18</sup>. For high Reynolds numbers, it is essentially impossible to resolve this phenomena using a conventional Eulerian description. The location where the eruption will occur is not known a priori; moreover due to the focusing nature of the phenomenon it is not possible to resolve the event using a mesh which is fixed in space. Recent progress in the development of Lagrangian algorithms to compute such flows is described by Peridier, Smith and Walker<sup>10</sup>.

The period required to induce an eruption for a given vortex is  $O(\kappa/a)$ ; thus an eruptive response occurs sooner for a stronger vortex and/or the closer the vortex is to the wall. Experiments<sup>15</sup> clearly show an eruptive response persists over a wide range of high Reynolds numbers and at least as low as  $R_v=10^4$ ; note that it is not a kinematical effect but an abrupt dynamical event which results in the discrete ejection of near-wall fluid.



Although all vortices carry the pressure signature that can provide an eruption, it is often argued<sup>9,11</sup> that hairpin vortices are the principal feature of turbulent flows near walls, for a variety of reasons. Hairpin vortices are low-speed streak creators<sup>3,11</sup> and are able to reproduce themselves. A schematic diagram of symmetric and asymmetric hairpin vortices is shown in figure 4. The symmetric hairpin vortex is the simplest mathematical model, although most hairpins in the turbulence will be asymmetric. There are two features of hairpin vortices which lead to their persistence in the flow. First, calculations show<sup>9</sup> (and experiments confirm<sup>11</sup>) that hairpins interact with a background shear flow to produce new subsidiary vortices to the side of the original hairpin vortex (see figure 4); in this manner the hairpin is able to multiply itself in the lateral direction. Secondly the vortex legs move progressively toward the wall as the vortex convects in a shear flow near the wall, thus hastening an eruptive response. Recent computations and well-controlled experiments<sup>9,11</sup> definitively show this occurs; in the region of adverse pressure gradient behind the vortex head and between the vortex legs, the creation of secondary hairpin vortices takes place through a viscous-inviscid interaction with the near-wall flow<sup>11</sup>. The process occurs after the vortex has convected over the wall for period of time and is characterized by a rapidly rising, narrow plume from the wall region; the plume then rolls over into a well-defined secondary vortex<sup>11</sup>.

## 6. Discussion

It has been argued that the equations governing the evolving wall-layer flow are of the boundary-layer type. To explain the production process in the near-wall region, it is necessary to isolate physical phenomena that lead to a strong interaction with the outer flow and which, in the process, destroy the local structure of the wall layer. Convected vortex motion above the wall layer (which is predominantly of the hairpin type) provides a moving zone of adverse pressure gradient. Note that the outer edge of the wall layer is not at some fixed value of  $y^+$ . Rather the boundary between the wall layer and outer region changes continually. In a sweep, the outer region penetrates close to the wall; conversely during a quiescent period the wall layer thickens continuously. When the vortex is strong enough and/or close enough to the wall an abrupt eruption will be produced; on the other hand, weaker disturbances can provoke an instability in the wall layer<sup>6</sup>. In either case, a local breakdown of the relatively well-ordered wall-layer flow occurs.

Finally, it is of interest to obtain an order of magnitude estimate of the period between bursts. For either the long wave problem discussed in §3 or the full three-dimensional problem described in §4, theoretical investigations<sup>10,12,13</sup> suggest that a moving disturbance, which imposes an  $O(1)$  adverse pressure gradient on the wall layer will provoke an eruption for  $T=O(1)$ ; it follows from equation (4) that this occurs for  $t=O(\nu\lambda^+/(u_\tau^2 W_1))$  and consequently

$$T_B^+ = O(\lambda^+/W_1) \quad . \quad (20)$$

The typical values give  $(\lambda^+/W_1)=50$ , which is of the same order as measured<sup>2</sup> values of  $T_B^+=110$ . As with most order of magnitude arguments, the estimate is not precise; however, it may be used to obtain a value for the characteristic length in the streamwise direction. Consider a convected vortex moving with speed  $O(U_1 U_\tau)$  at the outer edge of the wall layer; the mean time between bursts is  $T_B^+ \nu / u_\tau^2$  and may be regarded as the time required for the vortex to provoke an eruption. In this time period, the vortex

travels a distance  $L_x$  which may be adopted as the characteristic streamwise length and

$$L_x = U_1 u_\tau (T_B + \nu/u_\tau^2) \quad (21)$$

Using equation (20), it follows that  $L_x = 0(\lambda U_1/W_1)$  in agreement with equation (16).

Acknowledgements: This work was supported by the Air Force of Scientific Research under contract AFOSR-89-0065.

### References

1. Kline, S.J., Reynolds, W.C., Schraub, F.C. and Rundstadler, P.W., "The Structure of Turbulent Boundary Layers", J. Fluid Mech., Vol. 30, p. 133, 1967.
2. Walker, J.D.A., Abbott, D.E., Scharnhorst, R.K. and Weigand, G.G., "Wall-Layer Model for the Velocity Profile in Turbulent Flows", AIAA J., Vol. 72, Pt. 2, p. 140, 1989.
3. Acarlar, M.S. and Smith, C.R., "A Study of Hairpin Vortices in a Laminar Boundary Layer. Part 1. Hairpin Vortices Generated by Hemisphere Protruberances" and "Part 2. Hairpin Vortices Generated by Fluid Injection", J. Fluid Mech., Vol. 175, p. 1 and p. 43, 1987.
4. Hon, T.L. and Walker, J.D.A., "An Analysis of the Motion and Effects of Hairpin Vortices", Rept. FM-11, Dept. of Mech. Engrg. and Mech., Lehigh U., Bethlehem, PA; available NTIS-AD-A187261.
5. Smith, C.R. and Metzler, S.P., "The Characteristics of Low-Speed Streaks in the Near-Wall Region of a Turbulent Boundary Layer", J. Fluid Mech., Vol. 129, p. 27, 1983.
6. Walker, J.D.A. and Herzog, S., "Eruption Mechanisms for Turbulent Flows Near Walls", in Transport Phenomena in Turbulent Flows, M. Hirata and N. Kasagi (eds.), Hemisphere, p. 145, 1988.
7. Hatziaivramidis, D.T. and Hanratty, T.J., "The Representation of the Viscous Wall Region by a Regular Eddy Pattern", J. Fluid Mech., Vol. 95, p. 655, 1979.
8. Chapman, D.R. and Kuhn, G.D., "The Limiting Behavior of Turbulence Near a Wall", J. Fluid Mech., Vol. 170, p. 265, 1986.
9. Hon, T.L. and Walker, J.D.A., "Evolution of Hairpin Vortices in a Shear Flow", NASA Tech. Memo. 100858, ICOMP-88-9, 1988. Also to appear in Computers and Fluids.
10. Peridier, V., Smith, F.T. and Walker, J.D.A., "Methods for the Calculation of Unsteady Separation", AIAA Paper 88-0604, 26th Aerospace Sciences Meeting, Reno, NV, 1988.
11. Smith, C.R., Walker, J.D.A., Haidari, A.H. and Taylor, B.K., "Hairpin Vortices in Turbulent Boundary Layers; The Implications for Reducing Surface Drag", this volume, 1989.
12. Doligalski, T.L. and Walker, J.D.A., "The Boundary Layer Induced by a Convected Two-Dimensional Vortex", J. Fluid Mech., Vol. 139, p. 1, 1984.
13. Ersoy, S. and Walker, J.D.A., "Viscous Flow Induced by Counter-Rotating Vortices", Phys. Fluids, Vol. 28, p. 2687, 1985.
14. Ersoy, S. and Walker, J.D.A., "Flow Induced at a Wall by a Vortex Pair", AIAA J., Vol. 24, p. 1597, 1986.
15. Walker, J.D.A., Smith, C.R., Cerra, A.W. and Doligalski, T.L., "The Impact of a Vortex Ring on a Wall", J. Fluid Mech., Vol. 181, p. 99, 1987.
16. Ersoy, S. and Walker, J.D.A., "The Boundary Layer due to a Three-Dimensional Vortex Loop", J. Fluid Mech., Vol. 185, p. 569, 1987.

17. Chuang, F.J. and Conlisk, A.T., "The Effect of Interaction on a Boundary Layer Induced by a Convected Rectilinear Vortex", J. Fluid Mech., to appear.
18. Peridier, V., "Unsteady Vortex-Induced Separation", Ph.D. thesis, Lehigh U., 1989.

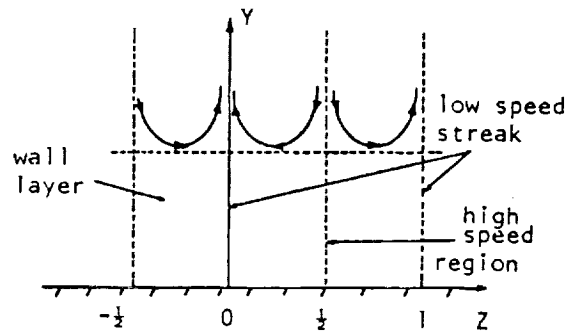


Figure 1. Assumed wall-layer structure during a quiescent period.

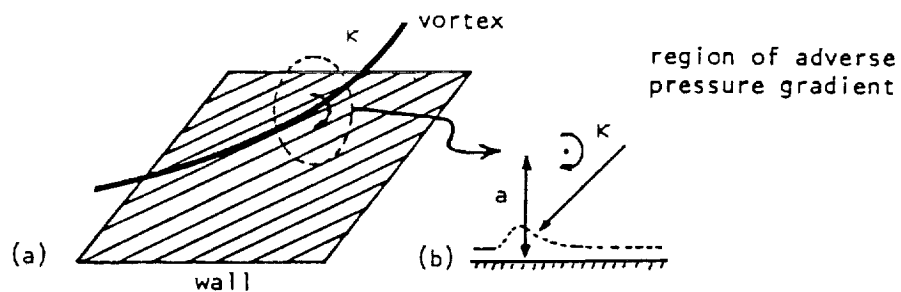


Figure 2. (a) Three dimensional vortex motion above a wall; (b) Details of a slice through the vortex.

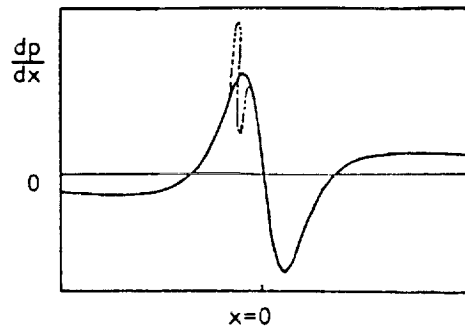


Figure 3. Pressure gradient near the wall due to a moving vortex.

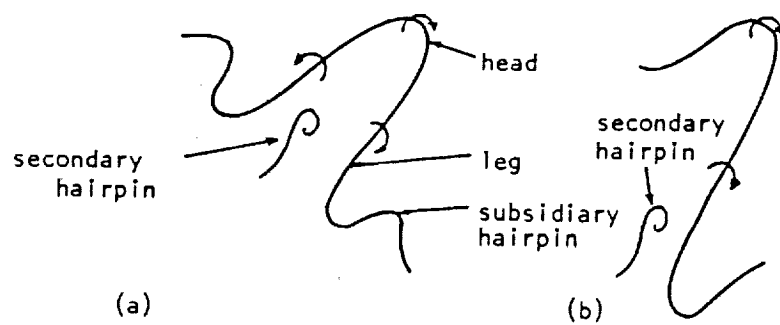


Figure 4. Schematic of (a) symmetric hairpin vortex; (b) asymmetric hairpin.

# Report Documentation Page

1. Report No. NASA TM-102362 ICOMP-89-26		2. Government Accession No.		3. Recipient's Catalog No.	
4. Title and Subtitle  Wall-Layer Eruptions in Turbulent Flows				5. Report Date	
				6. Performing Organization Code	
7. Author(s)  J.D.A. Walker				8. Performing Organization Report No.  E-5078	
				10. Work Unit No.  505-62-21	
9. Performing Organization Name and Address  National Aeronautics and Space Administration Lewis Research Center Cleveland, Ohio 44135-3191				11. Contract or Grant No.	
				13. Type of Report and Period Covered  Technical Memorandum	
12. Sponsoring Agency Name and Address  National Aeronautics and Space Administration Washington, D.C. 20546-0001				14. Sponsoring Agency Code	
15. Supplementary Notes  J.D.A. Walker, Lehigh University, Dept. of Mechanical Engineering and Mechanics, Bethlehem, Pennsylvania 18015 and Institute for Computational Mechanics in Propulsion, Lewis Research Center (work funded under Space Act Agreement C99066G). Space Act Monitor: Louis A. Povinelli.					
16. Abstract  The near-wall region of a turbulent flow is investigated in the limit of large Reynolds numbers. When low-speed streaks are present, the governing equations are shown to be of the boundary-layer type. Physical processes leading to local breakdown and a strong interaction with the outer region are considered. It is argued that convected vortices, predominantly of the hairpin type, will provoke eruptions and regenerative interactions with the outer region.					
17. Key Words (Suggested by Author(s))  Turbulent wall layer Turbulence production Turbulent bursts Low-speed streaks			18. Distribution Statement  Unclassified - Unlimited Subject Category 34		
19. Security Classif. (of this report)  Unclassified		20. Security Classif. (of this page)  Unclassified		21. No of pages  11	
				22. Price*  A03	

